

Evidence of electron correlations in plasmon dispersions of ultralow density two-dimensional electron systems

C. F. Hirjibehedin,^{1,2} A. Pinczuk,^{1,2,3} B. S. Dennis,² L. N. Pfeiffer,² and K. W. West²

¹*Department of Physics, Columbia University, New York, New York 10027*

²*Bell Labs, Lucent Technologies, Murray Hill, New Jersey 07974*

³*Department of Applied Physics and Applied Mathematics, Columbia University, New York, New York 10027*

(Received 30 January 2002; revised manuscript received 28 February 2002; published 15 April 2002)

Ultralow density two-dimensional electron systems are probed by inelastic light scattering at wave vectors large enough for both correlation and nonlocal effects to be significant. We find well-defined plasmons with dispersions that deviate from the “classical” \sqrt{q} limit. At lower temperatures, the deviation is negative and scales with the interparticle spacing and becomes positive as temperature increases. These results are interpreted as evidence of large correlation effects, arising from the predominance of electron interactions over nonlocal corrections at low temperatures.

DOI: 10.1103/PhysRevB.65.161309

PACS number(s): 73.20.Mf, 73.21.-b, 78.30.-j

The dominance of Coulomb interactions in electron systems can cause either classical or quantum phase transitions to highly correlated states,^{1,2} where the charge distribution in the electron system is dictated by electron interactions. There is much recent work in two dimensional (2D) systems on the possible existence of highly correlated states.³⁻⁶ A complete understanding of the low-temperature 2D ground state and definitive identification of novel quantum phases remains an actively pursued goal.⁶ When the kinetic energy of the system is well represented by the Fermi energy E_F , the impact of interactions is defined through the Coulomb energy $E_c = e^2/\epsilon a$ as $r_s = E_c/E_F = a/a_0^*$, where $2a = 2/\sqrt{\pi n}$ is the interparticle spacing and a_0^* is the effective Bohr radius. Above a critical r_s the 2D electron system may undergo a quantum phase transition to a broken symmetry state, such as a Wigner crystal.⁷ It is likely that correlation will change the electron distribution at length scales of the order of the interparticle spacing well before the system undergoes a phase transition. Experiments that probe strongly interacting electron systems at length scales of the order of the interparticle spacing may offer the insights that unambiguously identify correlations due to Coulomb interactions.

Here we report evidence of correlation in ultralow density 2D electron systems from inelastic light scattering studies of plasma oscillations. Light scattering experiments at laser wavelengths $\lambda_L \sim a$ reach wave vectors in the range of fundamental wave vectors: the Fermi wave vector $k_F = \sqrt{2\pi n}$; the Debye screening wave vector $k_D = 2\pi n e^2 / \epsilon k_B T$; and the Brillouin zone wave vector of a crystal phase,⁸ which is roughly $k_{BZ} = \pi/2a$. We find that determinations of plasmon dispersions probe electron interactions because the plasma frequency ω_p can be modified by correlation effects, which effectively reduce the Coulomb interactions, when the wave vector transfer $q \gtrsim 1/a$. Near these wave vectors, electron correlation from Coulomb interactions should manifest itself in negative higher order in q corrections to the plasmon dispersion.

Throughout our range of measurements, which extends to densities below 10^9 cm^{-2} and $a \gtrsim 0.18 \text{ }\mu\text{m}$, we find well-defined plasmon modes that disperse roughly according to

the lowest-order relation $\omega_p \sim \sqrt{q}$, with a negative correction that scales with r_s in the $T \rightarrow 0$ limit. These results are interpreted as manifestations of correlation from Coulomb interactions between electrons. At higher temperatures, competition with positive corrections from single-particle nonlocal effects⁹⁻¹³ determines the sign and magnitude of corrections to the lowest-order dispersion. These remarkable results extend to systems with large interaction strengths $r_s \sim 20$ for large wave vectors $q > 1/a$. Calculations of the plasmon dispersion that incorporate electron correlation^{14,15} show trends that are consistent with our results.

At the lowest densities and large r_s values, the determined correlation corrections are strong enough to be significant contributions to the plasmon energy at $q \sim k_{BZ}$. Because light scattering measurements in these ultra-low-density systems can reach wave vectors $q > k_{BZ}$, the periodicity of the mode dispersions can be used to identify crystal phases in ways that are analogous to Bragg scattering experiments. This is a particularly exciting prospect because the interaction strength in our lowest density sample is $r_s \sim 20$, which approaches the regime of r_s where Wigner crystallization is predicted to occur.⁷

The 2D electron systems examined here are formed in GaAs single quantum wells (SQWs), with well widths $w = 330 \text{ \AA}$. The SQWs are asymmetrically doped GaAs/Al_xGa_{1-x}As heterostructures with $0.03 > x > 0.01$. With modifications of previous designs,¹⁶ we have produced high-quality 2D electron systems with densities as low as $n = 7.7 \times 10^8 \text{ cm}^{-2}$. We shall discuss the results obtained from three such samples, which we denote as *A*, *B*, and *C*. These samples have electron densities (r_s values) of $4.0 \times 10^9 \text{ cm}^{-2}$ (8.7), $1.3 \times 10^9 \text{ cm}^{-2}$ (15.2), and $7.7 \times 10^8 \text{ cm}^{-2}$ (19.7), respectively. The density is determined for sample *A* from transport measurements of the quantum Hall effect¹⁷ and has an uncertainty of 1%. Reliable transport data are not available for the lower density systems because the sample designs are optimized for light-scattering measurements, making them difficult to contact electrically. The density in samples *B* and *C* is therefore determined by fitting the plasmon dispersion with Eq. (1), as described be-

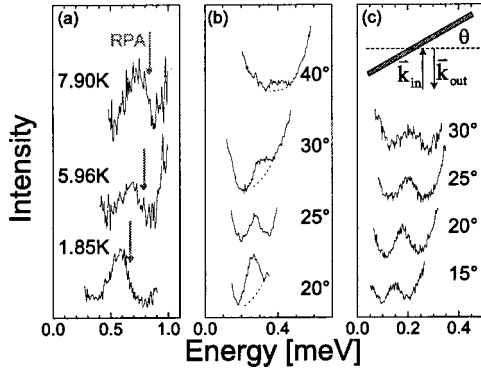


FIG. 1. Plasmon spectra from (a) sample A at various temperatures for a fixed wave vector $q = 1.18 \times 10^5 \text{ cm}^{-1}$, with the arrows indicating the values of ω_p predicted by RPA calculations (Refs. 10–12); (b) sample B at various angles at $T = 1.85 \text{ K}$, with dotted lines indicating an appropriate SQW photoluminescence background subtraction; (c) and sample C at various angles at 1.85 K (inset shows the backscattering geometry).

low; the uncertainty in these determinations is roughly 10%. The transport measurements of sample A show that the 2D system has a record high mobility $\mu = 9 \times 10^5 \text{ cm}^2/\text{Vs}$ at 15 mK. Previous attempts to reach this density range by gating higher-density samples^{18,19} have resulted in a decrease in mobility to below $10^5 \text{ cm}^2/\text{Vs}$.

Resonant inelastic light scattering spectra are obtained in a backscattering geometry, shown in the inset of Fig. 1(c). The wavelength of the incident photons is tuned close to the fundamental optical gap of the GaAs SQW. The incident power density is kept between $1.5 \times 10^{-1} \text{ W}/\text{cm}^2$ and $1 \times 10^{-3} \text{ W}/\text{cm}^2$ and no evidence of laser-induced heating is seen in these measurements. Samples are mounted in a liquid helium cryostat with windows for optical access, and are cooled either by immersion in liquid helium or by contact with helium vapor. The angle θ between the plane of the 2D electron system and the incident photons can be continuously tuned to define the q transferred to the 2D system, which for low-energy excitations can be written as $q = (4\pi/\lambda_L)\sin\theta$. We are able to acquire spectra at angles $\theta \leq 65^\circ$. This allows us to access wave vectors as large as $q = 1.4 \times 10^5 \text{ cm}^{-1}$, which for our densities can be close to k_D and significantly above $1/a$, and consequently k_F and k_{BZ} .

Figure 1 shows typical spectra from samples A, B, and C. In all three cases, the plasmons are well defined and dispersive. Figure 2 displays the dispersions measured at 1.85 K in the highest and lowest density systems, samples A and C, respectively. For sample A, the dispersion is reasonably described by the long-wavelength limit given by classical electrodynamics^{10–12,14,15}: $\omega_p = \omega_0 \equiv \sqrt{(2\pi n e^2 / \epsilon m^*)} q$, with $\epsilon = 13$ and $m^* = 0.067 m_0$. The dispersion in sample C, which has a record high $r_s = 19.7$ for a 2D electron system in GaAs, also seems to follow this $\omega_p \sim \sqrt{q}$ dependence even at wave vectors as large as $qa = 1.6$. This is remarkable because we expect significant deviations from this limit due to interaction effects that appear as higher order in q corrections. In this work, we consider three such effects. Correlation and the finite width of the electron layer both lower ω_p because they

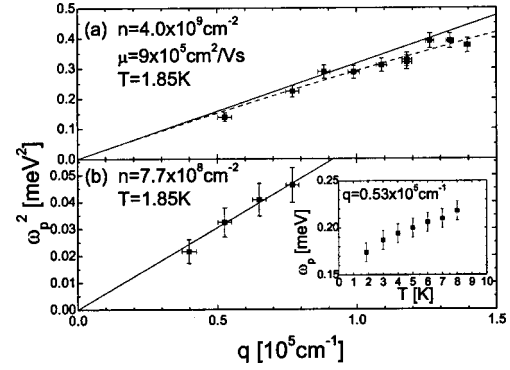


FIG. 2. (a) Plasmon dispersion from sample A (squares). The solid line shows the dispersion with $\xi = 0$, while the dashed line is a fit with $\xi = -0.089a$. (b) Dispersion from sample C (squares) with the best fit line for $\xi = 0$. The inset shows ω_p at various temperatures for $q = 0.53 \times 10^5 \text{ cm}^{-1}$.

effectively decrease the impact of the Coulomb interaction at large wave vectors. The former does so when $qa \geq 1$, while the latter may become apparent at $qw \geq 1$. The third and only positive correction comes from nonlocal effects, which are significant when $qv \sim \omega_0$, where v is the characteristic velocity of the electrons (the Fermi velocity $v_F = \hbar k_F / m^*$ at $T = 0$ and the thermal velocity $v_T = \sqrt{2k_B T / m^*}$ in the non-degenerate limit). To quantify the deviation, we write the plasmon dispersion beyond lowest order as

$$\omega_p^2 = \omega_0^2 [1 + \xi q], \quad (1)$$

where ξ is the strength of the first correction term. When higher-order effects such as correlation are significant, they will enter into the dispersion through ξ .

The behavior of ξ reveals significant negative corrections due to correlation. Consider first the results in Fig. 2(a) for the plasmon dispersion measured in the highest-density sample at $T = 1.85 \text{ K} = 1.1 T_F$, where $T_F = (1/k_B) E_F$, which is best described by Eq. (1) with a small negative correction: $\xi = -0.089a$. From the temperature dependence of ω_p shown in Fig. 1(a), it is also clear that ξ varies markedly with temperature, changing to a much larger $\xi = +0.386a$ at 7.90 K . The negative value of ξ is interpreted as evidence of the existence and impact of correlation effects on the plasmon dispersion. The change in sign of ξ at higher temperatures indicates that a large positive term attributed to nonlocal field corrections can become larger than correlation terms in the nondegenerate limit. Similar behavior of ξ is seen in the dispersion and temperature dependence of ω_p in sample C, shown in Fig. 2(b). Since finite width corrections are smaller and temperature independent, they cannot account for these trends (as discussed below).

The competition between correlation and nonlocal corrections to the plasmon dispersion is particularly well displayed in dispersions of the intermediate density sample B in Fig. 3. In this sample, the intermediate temperature ($T = 1.85 \text{ K}$) dispersion has very little deviation from the $\omega_p \sim \sqrt{q}$ behavior, and is well fit by $\xi = +0.009a$ for $n = 1.3 \times 10^9 \text{ cm}^{-2}$. This small value of ξ indicates that at this temperature the negative correlation and positive nonlocal corrections are

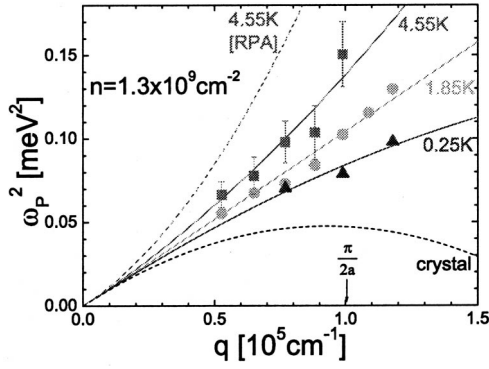


FIG. 3. Plasmon dispersion from sample *B* at 1.85 K (circles) and 4.55 K (squares); 250 mK measurements (triangles) by Eriksson *et al.*¹⁶ are also shown. Error bars are shown only on the 4.55 K data for clarity. The solid lines show the dispersions fit with $\xi = +0.009a$ at 1.85 K, $\xi = -0.116a$ at 0.25 K, and $\xi = +0.220a$ at 4.55 K. The upper dotted line shows the RPA calculation^{10–12} for the dispersion at 4.55 K, while the lower dotted line shows the dispersion for a crystal state with a hexagonal lattice.⁸ Also shown is the location of $k_{BZ} = \pi/2a$, the approximate location of the Brillouin zone wave vector.⁸

roughly equal in magnitude. At temperatures below T_F , the correlation correction dominates and the dispersion is well fit by a negative $\xi = -0.116a$. This behavior is reversed at higher temperatures, where the nonlocal effects are larger and the correction becomes $\xi = +0.220a$.

The $T \rightarrow 0$ behavior of ξ reveals further evidence of a correlation correction to ω_p . In Fig. 4, we show a summary of the ξ values obtained from the data in Figs. 1–3. For all three samples, ξ/a converges to nearly the same negative value at low temperatures, indicating that $\xi(T \rightarrow 0)$ scales close to linearly with $r_s \sim a$. Because the nonlocal correction⁹ is positive and very small in the low-temperature limit, it cannot be the dominant contribution to $\xi(T \rightarrow 0)$ at

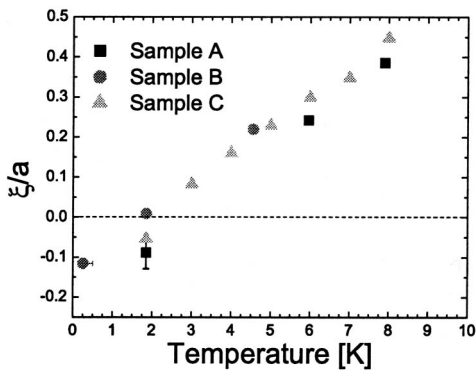


FIG. 4. Corrections to ω_p , as defined in Eq. (1), in units of the interparticle spacing from samples *A* ($4.0 \times 10^9 \text{ cm}^{-2}$), *B* ($1.3 \times 10^9 \text{ cm}^{-2}$), and *C* ($7.7 \times 10^8 \text{ cm}^{-2}$). For sample *B*, the values of ξ are based on fits of the dispersion, while the other values are based on temperature dependencies of ω_p at a fixed q . Characteristic error bars for ξ/a are shown on one point. An additional uncertainty in the temperature of the lowest temperature data point¹⁶ is also indicated. In the limit $T \rightarrow 0$, ξ scales with $a \sim r_s$, indicating that the behavior in this limit is driven by correlation.

ultra-low densities. Since negative finite width effects in low-density systems are expected to be independent of temperature and density to lowest order, they should not scale with r_s (and a). Further, it has been proposed that the combination of the finite width and nonlocal corrections in our 2D systems should have little impact at low temperatures because they should cancel almost exactly.¹⁵ We therefore interpret the limiting value

$$\xi(T \rightarrow 0) = -(0.17 \pm 0.04)a \quad (2)$$

as the negative correction to ω_p due to correlation effects.

The correction from nonlocal effects ξ_{NL} can be calculated within the random phase approximation (RPA).^{9–12} We find that in the two lowest density samples, the difference $\Delta\xi = \xi - \xi_{NL}$ becomes more negative with increasing T . Since correlation should weaken at higher T , we interpret this trend in $\Delta\xi$ as an evidence that RPA overstates the nonlocal correction to ω_p in large r_s systems. Further evidence of the discrepancy between the RPA and the plasmon dispersions measured by us can be seen in the 4.55 K dispersions shown in Fig. 3 and in the temperature dependence of sample *A* in Fig. 1(a).

Calculations of ω_p that include correlation effects are consistent with our results. Very recently, Hwang and Das Sarma¹⁵ have modified the RPA calculations to include correlation effects at finite temperatures through a variation of the Hubbard approximation. They calculate the correlation correction in the $T \rightarrow 0$ limit as $\xi_c = -a/2\sqrt{2} = 0.35a$. This calculation matches the scaling with the interparticle spacing observed in our results, but is a factor of two larger in strength. Hwang and Das Sarma find that their results are not significantly altered by using other methods to account for the static corrections, such as those based on the formalism developed by Singwi, Tosi, Land, and Sjolander²⁰ (STLS). A dynamic version of STLS may be more consistent with our results because the plasmon dispersions it generates lie between those from RPA and static STLS.²¹ In the nondegenerate regime we resort to a calculation that computes the plasmon dispersion in strongly coupled nondegenerate Coulomb liquids based on the physical model of quasilocalized particles occupying randomly located sites that are continuously rearranged.¹⁴ Within this formalism, $\xi = 3\lambda_D + D(q)$ where $3\lambda_D = 3k_D^{-1}$ is the nondegenerate, nonlocal correction and $D(q)$ is the pair-correlation function. Combined with numerical values from Monte Carlo simulations,²² this provides an explicit form for the correction in our region of interest: $\xi = 2a[(0.6906/\Gamma) + (0.1109/\Gamma^{3/4}) - 0.175]$, where $\Gamma = E_c/k_B T = a/2\lambda_D$ is the nondegenerate equivalent of r_s . The third term represents the $T \rightarrow 0$ limit of the correlation correction and is again consistent with the scale observed in our measurements but too large by a factor of two. We note that because our lowest-temperature measurements were done at $T \geq 0.5T_F$, we could find more pronounced effects of correlation at still lower temperatures.

At larger r_s and lower temperature, the systems may undergo a phase transformation and become fully correlated. By comparing the low-temperature dispersion in Fig. 3 to the expected phonon dispersion for a crystal of the same

density,⁸ we find that sample *B* has not yet entered this regime. The ability to make this comparison demonstrates that inelastic light scattering in ultralow density 2D systems, which can access $q \gtrsim k_{BZ}$, can differentiate between different ground-state phases. Also, as seen in Fig. 1(c), the plasmons should be easily resolved at $r_s = 37$ even though their energies will be roughly a factor of two lower.

Finally we note that inelastic light scattering also probes the damping of ultralow density 2D plasmons. As seen in Fig. 1, intensities of plasmons in these nondegenerate systems are very weak above a critical wave vector that is temperature dependent. These cutoffs, an example of which is seen in Fig. 1(b) to occur in sample *B* at 4.55 K for $q > 10^5 \text{ cm}^{-1}$, are roughly consistent with Landau damping,¹¹ which occurs when $\omega_p \sim qv_T$, where v_T is the average velocity of the electrons with energy $k_B T$. Before the cutoff the full width at half maximum (FWHM) of the plasmon increases with q and T . For all three samples at 1.85 K, we find that the width before the cutoff, corrected for instrumental broadening, is described by $\text{FWHM} = \alpha q$, where $\alpha = 1.2 \times 10^{-6} \text{ meV/cm}^{-1}$. This density and wave vector de-

pendence is consistent with collisional damping.¹² Similar results have also been seen recently in degenerate 2D systems by Nagao *et al.*²³

In summary, we have measured dispersive plasmon excitations of extremely dilute 2D electron systems with densities that extend below 10^9 cm^{-2} and $r_s \sim 20$. These experiments probe 2D systems at wave vectors that are large enough for correlation and nonlocal effects to be pronounced in the dispersions. We find well-defined plasmons whose energies at relatively large q and various T show evidence of being modified by correlation effects arising from the predominance of Coulomb interactions. Our results also demonstrate the ability of inelastic light scattering, which can access $q \gtrsim k_{BZ}$ in ultralow density systems, to identify quantum phase transitions to crystalline states predicted to occur because of strong interactions.

We wish to thank S. Das Sarma, A.J. Millis, S.H. Simon, and S. Syed for helpful discussions. This work was supported in part by the Nanoscale Science and Engineering Initiative of the National Science Foundation under NSF Award Number CHE-0117752.

¹E.P. Wigner, Phys. Rev. **46**, 1002 (1934).

²D. Ceperley, Nature (London) **397**, 386 (1999).

³H.W. Jiang, R.L. Willett, H.L. Stormer, D.C. Tsui, L.N. Pfeiffer, and K.W. West, Phys. Rev. Lett. **65**, 633 (1990).

⁴M.B. Santos, Y.W. Suen, M. Shayegan, Y.P. Li, L.W. Engel, and D.C. Tsui, Phys. Rev. Lett. **68**, 1188 (1992).

⁵H.A. Fertig, D.Z. Liu, and S. Das Sarma, Phys. Rev. Lett. **70**, 1545 (1993).

⁶E. Abrahams, S.V. Kravchenko, and M.P. Sarachik, Rev. Mod. Phys. **73**, 251 (2001).

⁷B. Tanatar and D.M. Ceperley, Phys. Rev. B **39**, 5005 (1989).

⁸L. Bonsall and A.A. Maradudin, Phys. Rev. B **15**, 1959 (1977).

⁹F. Stern, Phys. Rev. Lett. **18**, 546 (1967).

¹⁰A.L. Fetter, Phys. Rev. B **10**, 3739 (1974).

¹¹P.M. Platzman and N. Tzoar, Phys. Rev. B **13**, 3197 (1976).

¹²H. Totsuji, J. Phys. Soc. Jpn. **40**, 857 (1976).

¹³Unlike nonlocal exchange [e.g., J.C. Ryan, Phys. Rev. B **43**, 12 406 (1991)], these effects represent the energy needed to overcome the single-particle energy to create a collective mode.

¹⁴K.I. Golden, G. Kalman, and P. Wynn, Phys. Rev. A **41**, 6940 (1990).

¹⁵E.H. Hwang and S. Das Sarma, Phys. Rev. B **64**, 165409 (2001).

¹⁶M.A. Eriksson, A. Pinczuk, B.S. Dennis, C.F. Hirjibehedin, S.H. Simon, L.N. Pfeiffer, and K.W. West, Physica E (Amsterdam) **6**, 165 (2000).

¹⁷J. Zhu and H. L. Stormer (private communication).

¹⁸T. Sajoto, Y.W. Suen, L.W. Engel, M.B. Santos, and M. Shayegan, Phys. Rev. B **41**, 8449 (1990).

¹⁹H. Shtrikman, Y. Hanein, A. Soibel, and U. Meirav, J. Cryst. Growth **202**, 221 (1999).

²⁰K.S. Singwi, M.P. Tosi, R.H. Land, and A. Sjolander, Phys. Rev. **176**, 589 (1968).

²¹D. Neilson, L. Swierkowski, A. Sjolander, and J. Szymanski, Phys. Rev. B **44**, 6291 (1991).

²²H. Totsuji, Phys. Rev. A **17**, 399 (1978).

²³T. Nagao, T. Hildebrandt, M. Henzler, and S. Hasegawa, Phys. Rev. Lett. **86**, 5747 (2001).